with $a = 14.305$ Å, $b = 12.995$ Å, $c = 14.595$ Å, $\beta = 93.16°$, $V = 2709$ Å^3, and $Z = 8$.

A total of 4165 reflections were recorded on a Philips PW 1100 diffractometer in the θ–2θ scan mode with $2\theta = 6$–$46°$ using Mo Kα monochromatized radiation ($\lambda = 0.70926$ Å).

The unique reflections were used to solve the structure with MULTAN 78 programs. The 40 non-hydrogen atoms were anisotropically refined with block diagonal least squares ($R = 0.110$). All 36 hydrogen atoms were localized on a F map. The conventional R factor for the 3401 reflections considered observed with $I > 2\sigma(I)$ was 0.052.

X-ray Crystallographic Analysis for 55. The dimethyl ester crystallized in a monoclinic system, space group $P2_1/n$ (No. 14, centrosymmetric, racemate), with $a = 17.251$ Å, $b = 6.073$ Å, $c = 16.512$ Å, $\beta = 92.24°$, $V = 1729$ Å^3 and $Z = 4$.

A total of 3898 reflections were recorded on a Philips PW 1100 diffractometer in the θ–2θ scan mode with $2\theta = 6$–$52°$ using Mo Kα monochromatized radiation ($\lambda = 0.70926$ Å).

The unique reflections were used to solve the structure with MULTAN 77 programs. The 28 non-hydrogen atoms were anisotropically refined with block diagonal least squares ($R = 0.109$). All 24 hydrogen atoms were localized on a F map. The conventional R factor for the 2337 reflections considered observed with $I > 2\sigma(I)$ was 0.062.

Acknowledgment. P.R.S. thanks the Alexander von Humboldt Foundation for a fellowship. Financial support by the Deutsche Forschungsgemeinschaft, the Fonds der Chemischen Industrie, and the BASF AG as well as the large-scale preparation of intermediate **18** by the Ciba-Geigy AG are gratefully acknowledged. We express our appreciation to Dr. H. Fritz and Dr. D. Hunkler for NMR and to Dr. J. Wörth for MS measurements.

Registry No. 1, 89683-62-5; **3**, 465-73-6; **4**, 4723-74-4; **5**, 72448-17-0; **6**, 4309-87-9; **9**, 108590-43-8; **10**, 3647-99-2; **11**, 108510-50-5; **12**, 65879-03-0; **13**, 108510-51-6; **14**, 65879-05-2; **15**, 65879-04-1; **17**, 108510-52-7; **17** (C_s-symmetrical isomer), 108510-54-9; **18**, 65879-09-6; **19**, 108510-53-8; **21**, 65879-06-3; **26**, 108533-20-6; **27**, 1076-13-7; **30**, 108510-55-0; **31**, 3648-03-1; **32**, 3648-04-2; **40**, 65879-07-4; **42**, 65879-08-5; **48**, 89683-54-5; **49**, 89683-55-6; **50** (isomer 1), 108510-57-2; **50** (isomer 2), 108510-58-3; **51** (isomer 1), 89683-57-8; **51** (isomer 2), 89683-56-7; **52** (isomer 1), 108510-59-4; **52** (isomer 2), 108510-60-7; **53** (isomer 1), 89683-59-0; **53** (isomer 2), 89683-58-9; **55**, 89702-41-0; **56**, 89683-60-3; **57**, 107914-52-3; **58**, 108510-56-1; **59** (isomer 1), 108510-61-8; **59** (isomer 2), 108510-62-9; **60** (isomer 1), 108510-63-0; **60** (isomer 2), 108510-64-1; **61**, 108510-65-2; **62**, 108510-66-3; **63**, 108510-67-4; **64**, 89683-61-4; **65** (isomer 1), 108510-68-5; **65** (isomer 2), 108510-69-6; **66** (isomer 1), 108510-70-9; **66** (isomer 2), 108510-71-0; **68**, 108510-72-1; **69**, 108510-73-2; **70**, 107819-44-3; t-BuOCH(NMe_2)$_2$, 5815-08-7; MeSSMe, 624-92-0; maleic anhydride, 108-31-6; methyl formate, 107-31-3; benzaldehyde, 100-52-7.

An MC–SCF Study of the Mechanisms for 1,3-Dipolar Cycloadditions

Joseph J. W. McDouall,[†] Michael A. Robb,*[†] Ufuk Niazi,[†] Fernando Bernardi,[‡] and H. Bernhard Schlegel[⊥]

Contribution from the Department of Chemistry, King's College London, Strand, London WC2R 2LS, England, Departimento di Chimico 'G. Ciamician', Universita di Bologna, 40126 Bologna, Italy, and Chemistry Department, Wayne State University, Detroit, Michigan 48202. *Received December 9, 1986*

Abstract: MC–SCF gradient calculations are reported for three different 1,3-dipolar cycloaddition reactions—fulminic acid plus acetylene, fulminic acid plus ethylene, and nitrone plus ethylene. At the STO-3G and 4-31G basis set level, the concerted pathway is preferred over the concerted pathway involving a diradical intermediate. An alternative pathway leading to the oxime has also been studied, and these results give further support to the conjecture that the concerted mechanism is preferred.

The utility of 1,3-dipolar cycloaddition reactions in synthetic organic chemistry is well established; however, considerable controversy still surrounds the mechanism of these reactions.[1-4] Although 1,3-dipolar cycloadditions were introduced more than 25 years ago, experimental studies have been unable to choose conclusively between the synchronous, concerted mechanism proposed by Huisgen[1,3] and the stepwise, diradical path favored by Firestone.[2,4]

A variety of theoretical calculations have been performed on these systems over the past two decades. These have concerned themselves with problems of regioselectivity[5-15] or have treated only one mechanism.[12,13,16-18] Ab initio studies, which have treated both mechanisms, have also been unsuccessful in resolving this problem because of inadequate methodology.[19] In previous calculations, the closed-shell species involved in the concerted process and the open-shell (diradical) species encountered in the nonconcerted path could not be compared fairly, since the available methods artificially favored one path over the other. Unlike closed-shell, restricted Hartree–Fock (RHF) and open-shell, unrestricted Hartree–Fock (UHF) methods, the multiconfiguration

[†] King's College London.
[‡] Universita di Bologna.
[⊥] Wayne State University.

(1) Huisgen, R. *Angew. Chem.* **1963**, *2*, 565.
(2) Firestone, R. A. *J. Org. Chem.* **1968**, *33*, 2285.
(3) Huisgen, R. *J. Org. Chem.* **1976**, *41*, 403.
(4) Firestone, R. A. *Tetrahedron* **1977**, *33*, 3009.
(5) Fleming, I. *Frontier Molecular Orbitals and Organic Chemical Reactions*; Wiley and Sons: New York, 1976; p. 93.
(6) Fukui, K. *Molecular Orbitals in Chemistry, Physics and Biology*; Lowdin, P. O., *pullman*, B., Eds.; Academic Press: New York, 1964; p. 573.
(7) Hiberty, P. C.; Ohanessian, G. *J. Am. Chem. Soc.* **1982**, *104*, 66.
(8) Poppinger, D. *Aust. J. Chem.* **1976**, *29*, 465.
(9) Poppinger, D. *J. Am. Chem. Soc.* **1975**, *97*, 7486.
(10) Sustmann, R. *Tetrahedron Lett.* **1971**, 2721.
(11) Sustmann, R.; Trill, H. *Angew. Chem., Int. Ed. Engl.* **1972**, *11*, 838.
(12) Houk, K. N.; Sims, J. *J. Am. Chem. Soc.* **1973**, *95*, 3798.
(13) Houk, K. N.; Sims, J.; Duke, R. E., Jr.; Strozier, R. W.; George, J. K. *J. Am. Chem. Soc.* **1973**, *95*, 7287.
(14) Houk, K. N.; Sims, J.; Watts, C. R.; Luskus, T. J. *J. Am. Chem. soc.* **1973**, *95*, 7301.
(15) Houk, K. N. *Acc. Chem. Res.* **1975**, *8*, 361.
(16) Leroy, G.; Sana, M. *Tetrahedron* **1975**, *31*, 2091.
(17) Leroy, G.; Nguyen, M. T.; Sana, M. *Tetrahedron* **1978**, *34*, 2459.
(18) Komornicki, A.; Goddard, J. D.; Schaefer, H. F. *J. Am. Chem. Soc.* **1980**, *102*, 1763.
(19) Hiberty, P. C.; Ohanessian, G.; Schlegel, H. B. *J. Am. Chem. Soc.* **1983**, *105*, 719.

0002-7863/87/1509-4642$01.50/0

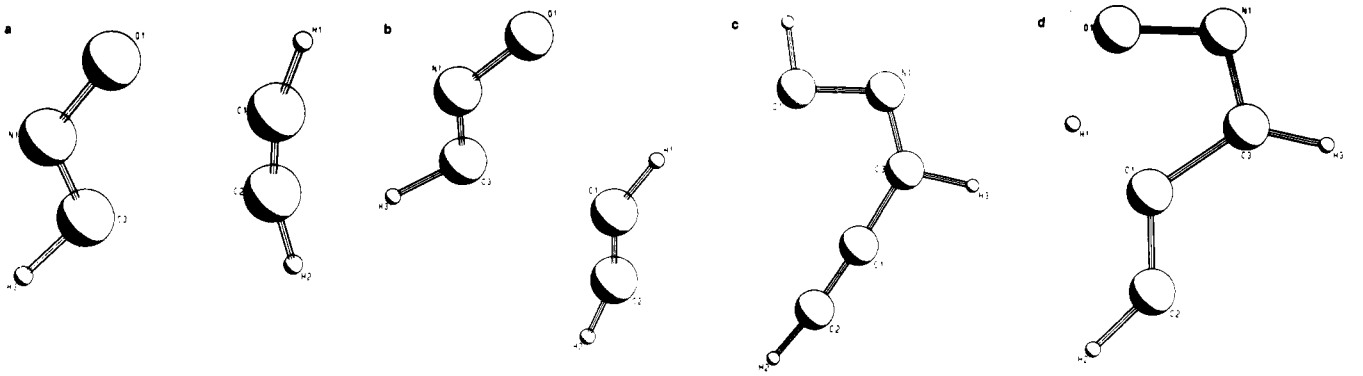

Figure 1. Schematic representation of the geometries for the reaction of fulminic acid with acetylene.

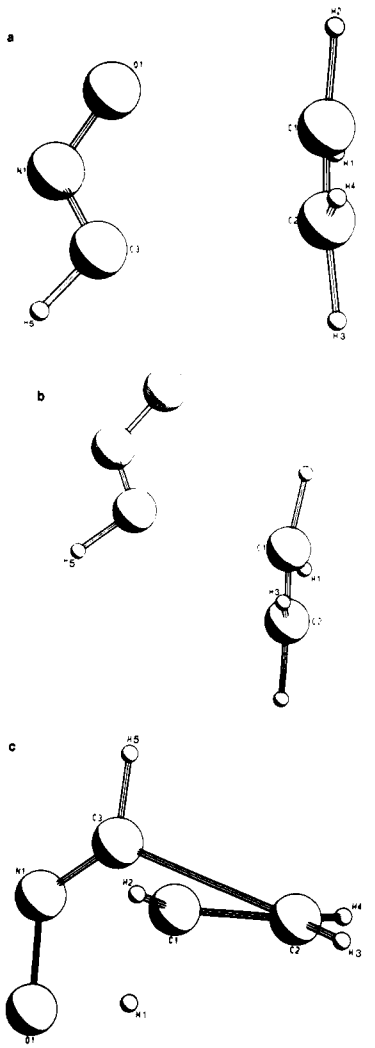

Figure 2. Schematic representation of the geometries for the reaction of fulminic acid with ethylene.

self-consistent-field (MCSCF) calculations[20] used in the present study can treat both mechanisms on an equal footing. In this work an investigation of the reaction surfaces was carried out with use of the MCSCF method with the standard STO-3G[21] and 4-31G[22] basis sets.

(20) (a) Eade, R. H. A.; Robb, M. A. *Chem. Phys. Lett.* **1981**, *83*, 362. (b) Schlegal, H. B.; Robb, M. A. *Chem. Phys. Lett.* **1982**, *93*, 43.
(21) Hehre, W. J.; Stewart, R. F.; Pople, J. A. *J. Chem. Phys.* **1969**, *51*, 2657.
(22) Ditchfield, R.; Hehre, W. J.; Pople, J. A. *J. Chem. Phys.* **1971**, *54*, 724.

Scheme I

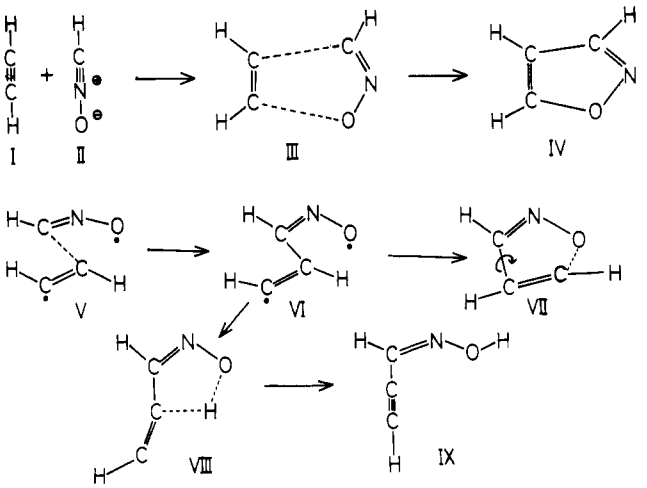

Table I. Fulminic Acid plus Acetylene

structure	absolute energy (Eh) STO-3G	absolute energy (Eh) 4-31G	rel energy (kcal/mol) STO-3G	rel energy (kcal/mol) 4-31G
I + II	-241.3130	-244.1360	0.0	0.0
III	-241.3056	-244.0946	4.6	26.0
IV	-241.5211	-244.2426	-130.6	-66.9
V	-241.2950	-244.0872	11.3	30.7
VI	-241.3746	-244.1246	-38.6	7.2
VII	-241.3636	-244.1123	-31.7	14.9
VIII	-241.3404	-244.1009	-17.2	22.0
IX	-241.4363	-244.2018	-77.4	-41.3

Results and Discussion

Concerted and nonconcerted pathways have been studied for three representative 1,3-dipolar cycloaddition reactions: (i) fulminic acid (HCNO) with acetylene to yield isoxazole, (ii) fulminic acid with ethylene to form 2-isoxazoline, and (iii) nitrone (CH_2NHO) with ethylene to yield isoxazolidine.

(i) Fulminic Acid + Acetylene → Isoxazole. In this example, both the 1,3-dipole and the dipolarophile have two sets of π orbitals, an in-plane and an out-of-plane set. The fulminic acid π orbitals are similar to those of an allyl system. The choice of valence space (i.e., the space of orbitals which are allowed to have variable occupancy) is central to the MCSCF method. It is important that all orbitals needed to describe a reaction are included. To choose these orbitals a simple procedure with single point CI calculations was adopted.

For a geometry resembling that of the concerted transition state, obtainable from previous calculations,[13,18] the two reacting moieties were moved apart to infinite separation and an MCSCF calculation was performed on all the π orbitals of the joint system, excluding the two lowest energy π orbitals of fulminic acid which were assumed to remain doubly occupied. This corresponded to an eight-electron/eight-orbital MCSCF calculation with a CI

Table II. Geometries for Fulminic Acid plus Acetylene

(a) reactants[a]			(b) product[a]			(c) cyclic transition state[a]		
	STO-3G	4-31G		STO-3G	4-31G		STO-3G	4-31G
H1–C1	1.07	1.05	H1–C1	1.08	1.06	H1–C1	1.07	1.05
C2–C1	1.18	1.20	C2–C1	1.33	1.33	C2–C1	1.20	1.22
H2–C2	1.07	1.05	H2–C2	1.08	1.06	H2–C2	1.07	1.05
O1–N1	1.28	1.26	O1–N1	1.39	1.42	O1–N1	1.32	1.25
C3–N1	1.17	1.14	O1–C1	1.41	1.38	O1–C1	2.21	2.28
H3–C3	1.06	1.05	C3–N1	1.31	1.29	C3–N1	1.24	1.20
N1–C3–H3	180.0	180.0	C3–C2	1.46	1.45	C3–C2	2.37	2.17
			H3–C3	1.08	1.06	H3–C3	1.09	1.06
			O1–N1–C3	107.0	105.8	O1–N1–C3	131.4	137.8
			H1–C1–C2	133.1	133.9	H1–C1–C2	167.1	169.6
			H1–C1–O1	116.5	116.4	H1–C1–O1	86.3	87.7
			C2–C1–O1	110.5	109.7	C2–C1–O1	106.6	102.7
			C1–C2–H2	129.1	128.8	C1–C2–H2	166.2	153.7
			C1–C2–C3	103.7	104.2	C1–C2–C3	102.1	104.7
			H2–C2–C3	127.1	127.1	H2–C2–C3	91.7	101.6
			N1–O1–C1	107.5	108.1	N1–O1–C1	101.8	94.9
			N1–C3–C2	111.3	112.2	N1–C3–C2	98.2	99.9
			N1–C3–H3	120.8	119.9	N1–C3–H3	125.4	137.3
			C2–C3–H3	127.9	127.9	C2–C3–H3	136.4	122.8

(d) first asynchronous transition state[b]			(e) extended diradical minimum (H1 and H2 in cis conformation)[b]			(f) extended diradical minimum (H1 and H2 in trans conformation)[b]		
	STO-3G	4-31G		STO-3G	4-31G		STO-3G	4-31G
H1–C1	1.07	1.07	H1–C1	1.09	1.08	H1–C1	1.08	1.07
C2–C1	1.21	1.24	C2–C1	1.30	1.31	C2–C1	1.30	1.30
H2–C2	1.07	1.06	H2–C2	1.11	1.08	H2–C2	1.08	1.07
O1–N1	1.32	1.23	O1–N1	1.38	1.33	O1–N1	1.38	1.33
C3–N1	1.25	1.21	C3–N1	1.29	1.26	C3–N1	1.29	1.26
C3–C1	2.13	1.92	C3–C1	1.49	1.46	C3–C1	1.52	1.49
H3–C3	1.09	1.06	H3–C3	1.09	1.07	H3–C3	1.09	1.07
O1–N1–C3	134.1	149.2	O1–N1–C3	114.8	120.1	O1–N1–C3	115.5	122.1
H1–C1–C2	150.3	140.2	H1–C1–C2	121.3	120.2	H1–C1–C2	121.1	120.6
H1–C1–C3	93.3	100.0	H1–C1–C3	116.0	116.9	H1–C1–C3	115.7	116.1
C2–C1–C3	116.4	119.8	C2–C1–C3	122.7	122.9	C2–C1–C3	123.2	123.3
C1–C2–H2	162.1	154.0	C1–C2–H2	132.7	136.8	C1–C2–H2	132.8	137.3
N1–C3–C1	118.8	113.1	N1–C3–C1	126.3	125.0	N1–C3–C1	126.4	125.2
N1–C3–H3	123.1	131.1	N1–C3–H3	115.9	116.6	N1–C3–H3	116.1	115.8
C1–C3–H3	118.1	115.8	C1–C3–H3	117.8	118.4	C1–C3–H3	117.5	119.1

(g) rotational transition state leading to product[b]			(h) oxime[c]			(j) transition state leading to oxime[d]		
	STO-3G	4-31G		STO-3G	4-31G		STO-3G	4-31G
C2–C1	1.30	1.31	N1–O1	1.41	1.41	N1–O1	1.39	1.37
H1–C1	1.08	1.07	H1–O1	1.03	0.97	H1–O1	1.42	1.52
H2–C2	1.09	1.08	C3–N1	1.29	1.26	C3–N1	1.29	1.26
C3–C2	1.54	1.50	H3–C3	1.09	1.07	H3–C3	1.09	1.07
N1–C3	1.28	1.26	C1–C3	1.46	1.42	C1–H1	1.25	1.26
O1–C1	3.45	3.53	C2–C1	1.19	1.20	C1–C3	1.49	1.46
O1–N1	1.38	1.33	H2–C2	1.07	1.05	C2–C1	1.26	1.26
H3–C3	1.09	1.07	N1–O1–H1	100.7	105.3	H2–C2	1.08	1.06
C2–C1–H1	132.3	133.0	O1–N1–C3	111.1	112.9	N1–O1–H1	96.3	95.2
C2–C1–O1	48.3	49.1	N1–C3–H3	116.2	114.9	O1–N1–C3	110.5	113.3
H1–C1–O1	136.0	138.1	N1–C3–C1	125.9	127.2	O1–H1–Cu	125.4	120.3
C1–C2–H2	121.6	120.5	H3–C3–C1	117.9	117.9	N1–C3–H3	121.2	120.8
C1–C2–C3	122.9	123.1	C3–C1–C2	178.8	177.3	N1–C3–C1	113.7	114.6
H2–C2–C3	115.6	116.4	C1–C2–H2	179.8	179.3	H3–C3–C1	125.1	124.6
C2–C3–N1	125.8	126.3				H1–C1–C3	94.0	96.8
C2–C3–H3	118.2	118.3				H1–C1–C2	127.7	124.8
N1–C3–H3	116.0	115.4				C3–C1–C2	138.3	138.3
C3–N1–O1	114.6	122.0				C1–C2–H2	144.2	152.2
C1–O1–N1	75.4	70.1						

[a] See Figure 1a for atom numbering. [b] See Figure 1b for atom numbering. [c] See Figure 1c for atom numbering. [d] See Figure 1d for atom numbering.

Table III. Fulminic Acid plus Ethylene

	absolute energy (Eh)		rel energy (kcal/mol)	
structure	STO-3G	4-31G	STO-3G	4-31G
I + II	−242.5435	−245.4093	0.0	0.0
III	−242.5393	−245.3633	2.6	28.8
IV	−242.7157	−245.4529	−108.0	−27.4
V	−242.5301	−245.3499	8.4	37.2
VI	−242.6036	−245.3640	−37.7	28.4
VIII	−242.5921	−245.3463	−30.5	39.5

space of 1764 configurations and yielded a set of orbitals localized onto the fragments. Then several single-point CI calculations were performed, using the re-orthogonalized fragment localized orbitals, bringing the two fragments closer to a plausible interfragment bond distance for the transition state. At each point the CI eigenvector showed that the out-of-plane π orbitals for both the acetylene and fulminic acid moieties remained essentially doubly occupied (in the case of the HOMO) or unoccupied (in the case of the LUMO), whereas the in-plane π orbitals showed marked HOMO to LUMO depopulation. From these data it was con-

Table IV. Geometries for Fulminic Acid plus Ethylene

(a) reactants[a]			(b) product[a]			(c) cyclic transition state[a]		
	STO-3G	4-31G		STO-3G	4-31G		STO-3G	4-31G
H1–C1	1.08	1.07	C2–C1	1.54	1.53	C2–C1	1.36	1.38
H2–C1	1.08	1.07	O1–C1	1.51	1.52	O1–C1	2.30	2.32
C2–C1	1.34	1.34	O1–N1	1.41	1.42	O1–N1	1.32	1.25
H3–C2	1.08	1.07	C3–C2	1.55	1.53	C3–C2	2.42	2.08
H4–C2	1.08	1.07	C3–N1	1.28	1.28	C3–N1	1.24	1.22
O1–N1	1.28	1.27	H3–C3	1.08	1.07	H3–C3	1.09	1.06
C3–N1	1.17	1.16	H1–C1	1.09	1.08	H1–C1	1.08	1.07
H5–C3	1.06	1.05	H2–C1	1.09	1.08	H2–C1	1.08	1.07
H1–C1–H2	116.2	116.2	H3–C2	1.09	1.08	H3–C2	1.08	1.07
H1–C1–C2	121.9	121.9	H4–C2	1.09	1.08	H4–C2	1.08	1.07
H2–C1–C2	121.9	121.9	C2–C1–O1	106.3	104.8	C2–C1–O1	104.2	100.0
C1–C2–H3	121.9	121.9	C2–C1–H1	112.9	113.9	C2–C1–H1	121.4	121.5
C1–C2–H4	121.9	121.9	C2–C1–H2	112.9	113.9	C2–C1–H2	121.4	121.5
H3–C2–H4	116.2	116.2	O1–C1–H1	107.7	106.4	O1–C1–H1	87.3	88.2
			O1–C1–H2	107.7	106.4	O1–C1–H2	87.3	88.2
			H1–C1–H2	109.1	110.7	H1–C1–H2	116.3	116.5
			C1–C2–C3	99.5	101.1	C1–C2–C3	99.9	103.5
			C1–C2–H3	112.9	112.9	C1–C2–H3	121.3	119.2
			C1–C2–H4	112.9	112.9	C1–C2–H4	121.3	119.2
			C3–C2–H3	111.4	110.7	C3–C2–H3	90.5	95.9
			C3–C2–H4	111.4	110.7	C3–C2–H4	90.5	95.9
			H3–C2–H4	108.6	108.4	H3–C2–H4	116.0	115.0
			O1–N1–C3	111.2	109.8	O1–N1–C3	133.1	135.4
			C1–O1–N1	108.1	109.2	C1–O1–N1	102.2	95.4
			C2–C3–N1	114.9	115.1	C2–C3–N1	100.6	105.7
			C2–C3–H3	124.1	125.2	C2–C3–H3	134.2	119.9
			N1–C3–H3	121.0	119.7	N1–C3–H3	125.2	134.5
(d) extended diradical transition state[b]			(e) extended biradical minimum[b]			(f) transition state leading to oxime[c]		
	STO-3G	4-31G		STO-3G	4-31G		STO-3G	4-31G
C2–C1	1.37	1.41	C2–C1	1.52	1.49	C2–C1	1.41	1.41
O1–N1	1.32	1.23	O1–N1	1.38	1.33	C3–C1	1.53	1.50
C3–C1	2.20	1.84	C3–C1	1.56	1.54	N1–C3	1.33	1.28
C3–N1	1.25	1.24	C3–N1	1.28	1.28	O1–N1	1.40	1.38
H3–C3	1.09	1.06	H3–C3	1.09	1.07	H3–C3	1.08	1.07
H1–C1	1.08	1.08	H1–C1	1.09	1.09	H2–C1	1.09	1.08
H2–C1	1.08	1.08	H2–C1	1.09	1.09	H1–C1	1.27	1.26
H3–C2	1.08	1.07	H3–C2	1.08	1.07	H1–O1	1.27	1.56
H4–C2	1.08	1.07	H4–C2	1.08	1.07	H3–C2	1.08	1.07
C2–C1–C3	107.9	110.4	C2–C1–C3	112.5	112.9	H4–C2	1.08	1.07
C2–C1–H1	119.9	116.8	C2–C1–H1	110.3	110.9	C2–C1–C3	119.8	119.0
C2–C1–H2	119.9	116.8	C2–C1–H2	110.3	110.9	C2–C1–H2	114.8	114.4
C3–C1–H1	92.1	98.6	C3–C1–H1	108.1	107.5	C2–C1–H1	112.7	112.1
C3–C1–H2	92.1	98.6	C3–C1–H2	108.1	107.5	C3–C1–H2	113.8	112.8
H1–C1–H2	115.1	112.3	H1–C1–H2	107.2	106.8	C3–C1–H1	88.3	93.5
C1–C2–H3	121.5	121.1	C1–C2–H3	117.7	120.7	H2–C1–H1	103.1	101.6
C1–C2–H4	121.5	121.1	C1–C2–H4	117.7	120.7	C1–C2–H3	121.0	121.0
H3–C2–H4	116.7	117.0	H3–C2–H4	115.8	118.1	C1–C2–H4	120.7	121.0
O1–N1–C3	134.8	143.9	O1–N1–C3	114.6	120.2	H3–C2–H4	117.0	117.3
C1–C3–N1	121.9	115.1	C1–C3–N1	125.4	123.9	C1–C3–N1	112.7	116.6
C1–C3–H3	115.6	119.5	C1–C3–H3	118.2	120.4	C1–C3–H3	126.0	124.1
N1–C3–H3	122.5	125.4	N1–C3–H3	116.3	115.7	N1–C3–H3	121.3	119.2
						C3–N1–O1	107.4	112.1
						N1–O1–H1	97.2	94.6
						C1–H1–O1	134.1	122.7

[a] See Figure 2a for atom numbering. [b] See Figure 2b for atom numbering. [c] See Figure 2c for atom numbering.

Table V. Nitrone plue Ethylene

structure	absolute energy (Eh)		rel energy (kcal/mol)	
	STO-3G	4-31G	STO-3G	4-31G
I + II	−243.7616	−246.5492	0.0	0.0
III	−243.7453	−246.5100	10.2	24.6
IV	−243.9024	−246.5831	−88.3	−21.2
V	−243.7416	−246.5019	12.5	29.7
VI	−243.8016	−246.5190	−25.1	19.0
V(gauche)	−234.7414	−243.4996	12.7	31.1
VI(gauche)	−243.8003	−246.5176	−24.3	19.8
VII	−243.7968	−246.5138	−22.1	22.2
VI–VI(gauche)	−243.7967	−246.5128	−22.1	22.8

cluded that the concerted mechanisms could be reliably described with only the in-plane π orbitals of both fragments.

A similar procedure was adopted for the diradical path and again the CI eigenvector showed no participation of the out-of-plane π orbitals. Consequently, all species for the fulminic acid/acetylene pair were calculated with a MCSCF valence space of four electrons in four orbitals, corresponding to the in-plane HOMO and LUMO of both fragments.

The two mechanisms for system i are shown in Scheme I. All structures were fully optimized at the MCSCF level with both the STO-3G and the 4-31G basis sets with use of analytic gradient methods.[20b] Transition structures were characterized by computing the Hessian for all internal coordinates by finite differences of gradients. The energies for reactants, transition structures, and products for this system are given in Table I. Some preliminary results for this reaction can be found in ref 23.

(23) Bernardi, F.; Bottoni, A.; McDouall, J. J. W.; Robb, M. A.; Schlegel, H. B. *Faraday Symp. Chem. Soc.* **1984**, *19* 137–147.

Table VI. Geometries for Nitrone plus Ethylene

(a) reactants[a]			(b) product[a]			(c) cyclic transition state[a]		
	STO-3G	4-31G		STO-3G	4-31G		STO-3G	4-31G
C2–C1	1.34	1.34	H1–C1	1.09	1.08	H1–C1	1.08	1.07
H1–C1	1.08	1.07	H2–C1	1.09	1.08	H2–C1	1.08	1.07
H2–C1	1.08	1.07	C2–C1	1.55	1.53	C2–C1	1.37	1.39
H3–C2	1.08	1.07	H3–C2	1.09	1.08	H3–C2	1.08	1.07
H4–C2	1.08	1.07	H4–C2	1.09	1.08	H4–C2	1.08	1.07
O1–N1	1.31	1.28	H5–N1	1.05	1.00	H5–N1	1.04	1.00
H5–N1	1.03	1.00	O1–C1	1.51	1.51	O1–C1	2.31	2.23
C3–N1	1.38	1.31	O1–N1	1.43	1.44	O1–N1	1.34	1.31
H6–C3	1.08	1.07	C3–C2	1.58	1.58	C3–C2	2.33	2.15
H7–C3	1.08	1.07	C3–N1	1.50	1.46	C3–N1	1.42	1.35
O1–N1–H5	116.8	115.0	H6–C3	1.09	1.08	H6–C3	1.09	1.07
O1–N1–C3	126.4	126.7	H7–C3	1.09	1.08	H7–C3	1.09	1.07
H5–N1–C3	116.9	118.3	H1–C1–H2	108.8	110.2	H1–C1–H2	116.3	116.0
C2–C1–H1	121.9	121.9	H1–C1–C2	111.9	113.0	H1–C1–C2	121.4	121.4
C2–C1–H2	121.9	121.9	H1–C1–O1	109.3	108.1	H1–C1–O1	87.7	89.2
H1–C1–H2	116.2	116.3	H2–C1–C2	112.9	114.2	H2–C1–C2	121.4	121.3
C1–C2–H3	121.9	121.9	H2–C1–O1	106.7	105.4	H2–C1–O1	88.2	89.9
C1–C2–H4	121.9	121.9	C2–C1–O1	107.0	105.5	C2–C1–O1	103.1	101.4
H3–C2–H4	116.2	116.3	C1–C2–H3	111.4	111.4	C1–C2–H3	120.7	119.4
N1–C3–H6	118.1	119.2	C1–C2–H4	112.3	112.4	C1–C2–H4	120.8	119.4
N1–C3–H7	118.9	118.4	C1–C2–C3	102.2	103.0	C1–C2–C3	101.8	101.8
H6–C3–H7	123.1	122.4	H3–C2–H4	108.7	108.3	H3–C2–H4	115.7	114.6
			H3–C2–C3	110.6	110.5	H3–C2–C3	92.7	97.7
			H4–C2–C3	111.4	111.1	H4–C2–C3	91.8	96.0
			H5–N1–O1	105.7	106.8	H5–N1–O1	113.7	114.8
			H5–N1–C3	106.0	113.4	H5–N1–C3	114.2	119.5
			O1–N1–C3	105.5	104.6	O1–N1–C3	118.5	117.9
			C1–O1–N1	106.5	107.0	C1–O1–N1	98.3	96.4
			C2–C3–N1	104.4	105.2	C2–C3–N1	96.5	98.5
			C2–C3–H6	113.1	113.0	C2–C3–H6	117.6	110.5
			C2–C3–H7	110.5	110.4	C2–C3–H7	96.9	94.5
			N1–C3–H6	110.2	110.2	N1–C3–H6	113.6	116.2
			N1–C3–H7	109.0	108.5	N1–C3–H7	114.3	115.7
			H6–C3–H7	109.4	109.4	H6–C3–H7	115.4	117.0
(d) extended diradical transition state $\rho = 183$[b]			(e) extended diradical transition state (gauche) $\rho = 120$[b]			(f) fragmentation transition state ($\rho = 82$) leading to gauche minimum[a]		
	STO-3G	4-31G		STO-3G	4-31G		STO-3G	4-31G
C3–C1	2.18	1.97	C3–C1	2.18	1.60	C3–C1	2.18	1.97
N1–C3	1.43	1.38	N1–C3	1.43	1.44	N1–C3	1.42	1.38
O1–N1	1.33	1.29	O1–N1	1.33	1.30	O1–N1	1.33	1.29
C2–C1	1.38	1.40	C2–C1	1.38	1.49	C2–C1	1.38	1.41
H1–C1	1.08	1.08	H1–C1	1.08	1.08	H1–C1	1.08	1.08
H2–C1	1.08	1.08	H2–C1	1.08	1.08	H2–C1	1.08	1.08
H3–C2	1.08	1.07	H3–C2	1.08	1.07	H3–C2	1.08	1.07
H4–C2	1.08	1.07	H4–C2	1.08	1.07	H4–C2	1.08	1.07
H5–C3	1.09	1.07	H5–C3	1.09	1.08	H5–C3	1.09	1.07
H6–C3	1.09	1.07	H6–C3	1.09	1.08	H6–C3	1.09	1.07
H7–N1	1.03	1.00	H7–N1	1.03	0.99	H7–N1	1.03	0.99
C3–C1–C2	108.4	110.8	C3–C1–C2	109.3	113.7	C3–C1–C2	110.5	113.4
C3–C1–H1	94.0	98.8	C3–C1–H1	93.5	106.8	C3–C1–H1	92.7	94.4
C3–C1–H2	92.6	94.4	C3–C1–H2	93.4	107.7	C3–C1–H2	92.2	97.5
C2–C1–H1	119.2	117.1	C2–C1–H1	119.3	111.0	C2–C1–H1	119.3	117.7
C2–C1–H2	119.5	118.1	C2–C1–H2	119.0	110.3	C2–C1–H2	119.1	116.5
H1–C1–H2	114.8	113.1	H1–C1–H2	114.6	107.0	H1–C1–H2	114.9	113.1
C1–C3–N1	110.6	108.3	C1–C3–N1	111.6	113.6	C1–C3–N1	112.6	110.7
C1–C3–H5	103.6	104.6	C1–C3–H5	105.0	110.0	C1–C3–H5	104.0	105.2
C1–C3–H6	102.1	101.0	C1–C3–H6	100.4	109.2	C1–C3–H6	99.8	98.8
N1–C3–H5	112.3	113.5	N1–C3–H5	112.0	107.6	N1–C3–H5	112.4	113.4
N1–C3–H6	112.8	113.0	N1–C3–H6	112.7	108.1	N1–C3–H6	112.7	112.6
H5–C3–H6	114.5	115.1	H5–C3–H6	114.2	108.3	H5–C3–H6	114.5	114.8
C3–N1–O1	122.4	122.7	C3–N1–O1	122.4	119.4	C3–N1–O1	122.4	122.6
C3–N1–H7	116.0	120.1	C3–N1–H7	115.9	121.7	C3–N1–H7	116.1	120.3
O1–N1–H7	115.3	115.8	O1–N1–H7	115.3	116.1	O1–N1–H7	115.3	115.9
C1–C2–H3	121.4	121.4	C1–C2–H3	121.4	120.5	C1–C2–H3	121.4	121.3
C1–C2–H4	121.4	121.2	C1–C2–H4	121.4	120.8	C1–C2–H4	121.4	121.3
H3–C2–H4	116.6	116.8	H3–C2–H4	116.6	117.3	H3–C2–H4	116.6	116.8
(g) extended diradical transition state ($\rho = 46$) closes to product[b]			(h) extended diradical minimum $\rho = 181$[b]			(j) extended diradical minimum (gauche) $\rho = 66$[b]		
	STO-3G	4-31G		STO-3G	4-31G		STO-3G	4-31G
C3–C1	1.59	1.58	C3–C1	1.59	1.58	C3–C1	1.59	1.58
N1–C3	1.50	1.45	N1–C3	1.49	1.44	N1–C3	1.49	1.44
O1–N1	1.38	1.31	O1–N1	1.38	1.30	O1–N1	1.38	1.31
C2–C1	1.51	1.49	C2–C1	1.52	1.49	C2–C1	1.52	1.49

Table VI (Continued)

(g) extended diradical transition state (ρ = 46) closes to product[b]			(h) extended diradical minimum ρ = 181[b]			(j) extended diradical minimum (gauche) ρ = 66[b]		
	STO-3G	4-31G		STO-3G	4-31G		STO-3G	4-31G
H1-C1	1.09	1.08	H1-C1	1.09	1.08	H1-C1	1.09	1.08
H2-C1	1.09	1.09	H2-C1	1.09	1.08	H2-C1	1.09	1.08
H3-C2	1.08	1.07	H3-C2	1.08	1.07	H3-C2	1.08	1.07
H4-C2	1.08	1.07	H4-C2	1.08	1.07	H4-C2	1.08	1.07
H5-C3	1.09	1.08	H5-C3	1.09	1.08	H5-C3	1.09	1.08
H6-C3	1.09	1.08	H6-C3	1.09	1.08	H6-C3	1.09	1.08
H7-N1	1.04	0.99	H7-N1	1.04	0.99	H7-N1	1.04	0.99
C3-C1-C2	113.5	113.9	C3-C1-C2	111.8	112.4	C3-C1-C2	113.6	113.7
C3-C1-H1	108.4	108.2	C3-C1-H1	108.4	108.0	C3-C1-H1	107.9	107.1
C3-C1-H2	107.0	105.9	C3-C1-H2	108.0	106.6	C3-C1-H2	107.1	107.0
C2-C1-H1	109.8	109.9	C2-C1-H1	110.2	110.9	C2-C1-H1	110.3	110.8
C2-C1-H2	110.3	111.3	C2-C1-H2	110.3	111.2	C2-C1-H2	109.8	110.4
H1-C1-H2	107.7	107.3	H1-C1-H2	108.0	107.6	H1-C1-H2	107.9	107.5
C1-C3-N1	113.5	112.1	C1-C3-N1	113.7	112.5	C1-C3-N1	114.7	113.4
C1-C3-H5	110.0	109.8	C1-C3-H5	109.6	109.9	C1-C3-H5	109.6	109.9
C1-C3-H6	108.5	108.1	C1-C3-H6	109.5	109.3	C1-C3-H6	108.7	109.1
N1-C3-H5	107.5	107.8	N1-C3-H5	107.5	108.2	N1-C3-H5	107.7	108.1
N1-C3-H6	109.0	110.6	N1-C3-H6	107.8	108.2	N1-C3-H6	107.4	107.8
H5-C3-H6	108.2	108.4	H5-C3-H6	108.6	108.6	H5-C3-H6	108.5	108.5
C3-N1-O1	112.3	118.0	C3-N1-O1	112.9	119.1	C3-N1-O1	112.7	119.2
C3-N1-H7	109.5	120.3	C3-N1-H7	110.0	121.6	C3-N1-H7	110.3	122.1
O1-N1-H7	108.4	114.7	O1-N1-H7	109.2	115.9	O1-N1-H7	109.1	116.2
C1-C2-H3	119.6	121.1	C1-C2-H3	117.9	121.0	C1-C2-H3	118.4	120.9
C1-C2-H4	118.8	120.8	C1-C2-H4	117.7	120.4	C1-C2-H4	117.9	120.5
H3-C2-H4	116.7	118.1	H3-C2-H4	115.6	117.5	H3-C2-H4	115.7	117.7

[a] See Figure 3a for atom numbering. [b] See Figure 3b for atom numbering.

Table VII. Activation Barriers Predicted Using Multireference CI with 4-31G Basis (See Text for Details)

	case i	case ii	case iii
Absolute Energy (Eh)			
reactants	−244.2175	−245.4155	−246.5978
concerted transition state	−244.1884	−245.3911	−246.5787
diradicaloid transition state	−244.1670	−245.3621	−246.5554
Relative Energy (kcal/mol)			
reactants	0.0	0.0	0.0
concerted transition state	18.2	15.3	11.9
diradicaloid transition state	31.7	33.5	26.6

For the addition of fulminic acid to acetylene, stationary points were found for the concerted path (I + II → III → IV) and a nonconcerted path (I + II → V → VI → VII → IV) involving a diradical intermediate, VI. The first transition state of the nonconcerted path, V, is the highest energy structure along this path and so will be rate-determining. At the STO-3G level, the transition structure for the concerted path, III, is approximately 7 kcal/mol lower than the transition structure for the nonconcerted path, V. This result is confirmed at the 4-31G level, where the concerted path is 5 kcal/mol lower. This suggests that in the gas phase, the two processes are close enough in energy to be competitive but that the concerted path will be preferred.

An additional piece of experimental evidence lends some support to these results. The products of 1,3-dipolar additions are not exclusively heterocycles; small quantities of the oxime, IX, are formed as well.[24] The reaction path leading to the oxime must pass through the diradical intermediate (I + II → V → VI → VIII → IX). At the 4-31G level, VIII, the transition structure connecting the diradical intermediate with the oxime is 7 kcal/mol higher than VII, the transition structure for closure to the cyclic product. Nevertheless, the oxime transition structure, VIII, is 9 kcal/mol lower than V, the first transition state of the nonconcerted path. If the nonconcerted path were favored experimentally, a greater proportion of the oxime product would be expected, since the activation energy for the first transition state would provide enough energy for the system to form either the heterocycle, IV, or the oxime, IX.

It should be mentioned that considerable effort was made to locate an envelope-type concerted transition state for this system, as advocated by Huisgen.[3] All attempts to locate such a structure resulted in relaxation back to the planar structure.

The energies and geometries for the various structures obtained for this example are tabulated in Tables I and II, respectively, and a schematic representation of the structure is given in Figure 1. The principal difference between the structures obtained for the first diradicaloid transition structure here and in ref 19 is that the hydrogen atoms on the acetylene moiety are in a trans conformation to each other, whereas in ref 19 they appear in a cis conformation. Attempts to locate a cis transition structures were not successful.

(ii) Fulminic Acid + Ethylene → 2-Isoxazoline. In this case the dipolarophile, ethylene, has only one set of π orbitals. The same procedure for choosing the valance space as described for case i was adopted. With STO-3G basis set, calculations were carried out with a four-electron/four-orbital valence space in the manner of the first example. At the 4-31G level, it was found that the convergence of the MCSCF wave function was affected by a near degeneracy between the in-plane and out-of-plane π systems of fulminic acid. Thus for this technical reason, the 4-31G optimizations were performed with the HOMO and LUMO of the out-of-plane π system included in the valence space. This yields a six-electron/six-orbital MCSCF calculation with a CI space of 175 configurations. It must be emphasized that the inclusion of the two extra orbitals in the valence space was purely to improve convergence of the MCSCF calculations.

The results are similar to those obtained for case i. At the STO-3G level, the transition structure for the concerted path is 6 kcal/mol lower than the transition structure for formation of the diradical. This is confirmed at the 4-31G level, the difference being 8 kcal/mol. Attempts to locate a transition structure connecting the diradical intermediate with the cyclic product have been unsuccessful. However, a transition structure connecting the diradical minimum with the oxime was located at both the STO-3G and 4-31G levels.

The energies and geometries for the structures obtained for this example are tabulated in Tables III and IV, respectively, and a schematic representation of the structures is given in Figure 2.

(iii) Nitrone + Ethylene → Isoxazolidine. In this final example, both the dipole annd the dipolarophile have only one set of π orbitals. hence the choice of the π space is clear. All the calculations for this dipole/dipolarophile pair were performed with a four-electron/four-orbital valance space.

(24) Harcourt, R. D.; Little, R. D *J. Am. Chem. Soc.* **1984**, *106*, 41.

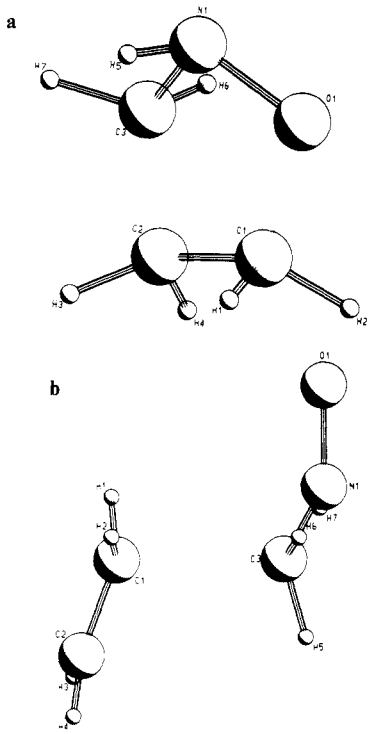

Figure 3. Schematic representation of the geometries for the reaction of Nitrone with ethylene.

The surface for this reaction is slightly more complicated than that of the first two examples due to the existence of various conformational isomers of the intermediates and transition structures. Two diradical minima exist, the first of which is a planar structure with a dihedral angle ρ, between the plane containing the two carbon atoms of ethylene and the plane containing the carbon and oxygen atoms of nitrone, of approximately 180°. In the second diradical minimum (gauche) the angle ρ is approximately 66°. These two minima are connected by a transition state (gauche) that differs from the two minima essentially in the value of ρ alone (approximately 120°). The gauche diradical minimum connects with the cyclic product via a transition state with a value for ρ of approximately 46°. The gauche diradical minimum can also be formed via a fragmentation-type transition state with a long interfragment bond. Closure to the product can take place by a positive rotation of the first diradical minimum (ρ positive) or by a negative rotation (ρ negative). The two paths will be slightly different because the structures are nonplanar. Both paths have been located and are very similar, but for reasons of space only one path has been documented here.

The results for this example confirm those obtained for the first two examples. The concerted path is favored by 2 kcal/mol at the STO-3G level and 5 kcal/mol at the 4-31G level.

The energies and geometries for the structures obtained for this example are tabulated in Tables V and VI, respectively, and a schematic representation of the structures is given in Figure 3. The geometry for the concerted transition state Table VIc is rather different than that found in ref 17 because even the concerted mechanism has some diradical character in this case.

Correlated Energy Predictions

Activation barriers have been calculated for all three cases with a large multireference CI with the 4-31G basis and the MCSCF/4-31G geometries. In each case a reference space of 20 configuration state functions was used. A "first-order CI space" was generated from the 20 configuration reference space. This consisted of all configurations with at most one occupied virtual orbital, one core/inactive hole (or vacancy), and all possible valance/active orbital occupancies with the 1s and 2s doubly occupied orbitals of all heteroatoms being held frozen. Such a CI space includes the most important double excitations where one have a core-virtual single excitation coupled with a valence–valence single excitation and recovers the strongly structure dependent semi-internal electron correlation. This yielded configuration spaces for the three examples of (case i) 7270 configurations, (case ii) 9170 configurations, and (case iii) 11280 configurations. In each case the harmonic level truncation scheme proposed by Hegarty and Robb[25] was employed (for details of the implementation see ref 26) with a harmonic level difference of three.

The space of reference configurations was chosen to be that of the MCSCF calculations reported above for cases i and iii. For case ii, only the in-plane π system was used in generating the reference space. This was felt to be valid since the out-of-plane π system was incorporated into the MCSCF calculations solely to improve convergence.

The experimental activation barriers for the three examples studied here are not known. However, ref 18 states that Huisgen has estimated the activation barrier for case i to be 8–12 kcal/mol. From ref 4, typical reaction barriers obtained experimentally for a variety of 1,3-dipolar cycloadditions lie in the range of 8–18 kcal/mol. At present these are the only guidelines known to us for comparison with experiment.

The results obtained are given in Table VII. In all cases the concerted process has a significantly lower activation barrier than the diradical path. The concerted transition state is lower in energy than the first diradicaloid transiton state by (case i) 13.4 kcal/mol, (case ii) 18.2 kcal/mol, and (case iii) 14.7 kcal/mol. The activation barriers predicted for the concerted process—(case i) 18.2 kcal/mol, (case ii) 15.3 kcal/mol, and (case iii) 11.9 kcal/mol—can be seen to lie in the experimental range of 8–18 kcal/mol. In contrast, the activation energies for the diradical path are predicted to be significantly higher than typical experimental values.

Conclusion

The present MCSCF and higher level correlated calculations on the three representative 1,3-dipolar cycloadditions indicate that the concerted path is preferred since it has a significantly lower barrier to activation than the diradical path. Furthermore, unlike the diradical path, the predicted activation barriers for the concerted process lie in the correct experimental range. However, this does not exclude the possibility of traversing the diradical path as indicated by the experimental observation that the oxime is formed in small quantities.

Acknowledgment. This work has been supported in part from Grant GR/D/23305 from the Science Research Council (UK) and by contract ST2J-0083-2-UK from the EEC. The MC-SCF gradient programs were developed under NATO Grant RG 096.81 and have been interfaced with the GAUSSIAN 80 suite[27] of programs.

Registry No. Fulminic, 506-85-4; acetylene, 74-86-2; ethylene, 74-85-1; nitrone, 463-62-7.

(25) Hegarty, D.; Robb, M. A. *Mol. Phys.* **1979**, *38*, 1795.
(26) Niazi, U.; Robb, M. A. *Comput. Phys. Rep.* **1984**, *1*, 127.
(27) Binkley, J. S.; Whiteside, R. A.; Krishnan, R.; Seeger, R.; Defrees, D. J., Schlegel, H. B.; Topial, S.; Kahn, L. R.; Pople J. A. *QCPE* **1981**, *13*, 406.